Asian Journal of Chemistry; Vol. 37, No. 8 (2025), 1861-1866

ASIAN JOURNAL OF CHEMISTRY

https://doi.org/10.14233/ajchem.2025.33996

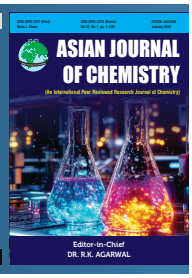


# Antibacterial and Anticancer Activities of Naturally Derived Nano Calcium Carbonate for Biomedical Applications

E. THENPANDIYAN[1], V. RAMASAMY[2,*], G. SURESH[3], S. SENTHIL[4] and T. SATHISHPRIYA[5]

[1]Department of Physics, Academy of Maritime Education and Training, Kanathur, Chennai-603112, India
[2]Department of Physics, Annamalai University, Annamalai Nagar-608002, India
[3]Department of Humanities and Science/Physics, Centre for Nanotechnology Research, Aarupadai Veedu Institute of Technology, Vinayaka Mission's Research Foundation (DU), Chennai-603104, India
[4]Department of Physics, Panimalar Engineering College, Poonamallee, Chennai-600123, India
[5]Department of Science & Humanities (Physics), Loyola Institute of Technology, Palanchur, Chennai-600123, India

*Corresponding author: E-mail: srsaranram@rediffmail.com

*Received*: 6 May 2025; *Accepted*: 29 June 2025; *Published online*: 31 July 2025; AJC-22062

Pristine $CaCO_3$ nanoparticles was synthesized through an eco-friendly biomimetic route using a natural calcium carbonate source of $CaMg(CO_3)_2$ (dolomite rock). The physico-chemical properties of prepared $CaCO_3$ nanoparticles were assessed using FTIR, XRD, FE-SEM, HR-TEM and XPS analyses. The presence of the functional groups through FTIR analysis confirmed the presence of $CaCO_3$ (calcite polymorph) in the synthesized sample. The occurrence of rhombohedral $CaCO_3$ with a well-crystalline nature was confirmed through XRD pattern and calculated crystallite size is about 25 nm. The FE-SEM and HR-TEM analyses exhibit the spherical with few rhombohedral like morphology. The presence of binding energies of Ca, O and C confirms that the synthesized sample is in the pure form of $CaCO_3$. The biomedical activities of prepared $CaCO_3$ nanoparticles were examined through antibacterial and anticancer activities using Gram-positive (*Staphylococcus aureus*) and Gram-negative bacteria (*Salmonella* sp.) and the human breast cancer cell line MCF-7. These results show that $CaCO_3$ nanoparticles act as good antibacterial agents. The cytotoxicity effect of $CaCO_3$ nanoparticles on MCF-7 is 18% cell viability at 1000 µg/mL. The calculated $IC_{50}$ value of $CaCO_3$ nanoparticles against MCF-7 is 229.10 µg/mL. These results show that the naturally derived $CaCO_3$ nanoparticles are potent anticancer drugs against human breast cancer cell lines.

**Keywords: Dolomite rock, Nano $CaCO_3$, *Staphylococcus aureus*, *Salmonella* sp., MCF-7.**

## INTRODUCTION

Calcium carbonate ($CaCO_3$) is one of the most abundant inorganic biominerals in nature, typically extracted from limestone sedimentary rock. It has been used in various applications such as paint, oil, plastics, drug delivery, templates for microcapsules, coatings, eco-friendly items like paper, bone filling material and calcium enriched foods [1] becuase of its biocompatibility, large specific area, hierarchical structure mesoporosity and low cost [2,3]. Specifically in biomedical fields, it can be utilized in the treatment of hyper phosphatemia (chronic renal failure) by means of a phosphate binder, a low-cost nutritional calcium supple mentor gastric antacid, an inactive plaster for drugs and other medicines, in the making of toothpaste, colour retainer and a food preservative [4].

Nowadays, in nanomedicine applications, metal oxide-based nanoparticles (titanium, platinum, copper, gold, iron, silver, *etc.*) play a major role. Specifically, $CaCO_3$ nanoparticles attract the researchers because of their easy preparation, biodegradability and excellent biocompatibility. In drug delivery field, it can be used in various treatments such as photothermal therapy (PTT)/photodynamic therapy (PDT), immune therapy, gene therapy and chemical therapy [5,6]. Thus, it is thought that nano $CaCO_3$ based drug delivery systems exhibits excellent biocompatibility [5,7]. The calcium carbonate and calcium phosphate are the major constituents of animal bones and teeth. In order to apply nano $CaCO_3$ in to the above said biomedical applications, the present material needs to be checked against bacteria and cancer activities.

Interestingly, the biomedical applications of $CaCO_3$ nanoparticles could be varied with sources. The important natural sources are dolomite, limestone, corals, pearls, chalk and marbles, egg and mollusk shells [8]. Among these, dolomite is an another supportable source to synthesize the calcium carbonate since dolomite ($CaMg(CO_3)_2$) represents a significant part of the sedimentary rocks [9], which are plenty available in India. Therefore, turning this dolomite rock into $CaCO_3$ would be noticeably economical and eco-friendly process through easy and efficient biomimetic synthesis which attracts the researchers over other methods (microwave solid-state, precipitation, atomized microemulsion, hydrothermal, mechanochemical, co-precipitation and sol-gel synthesis.

The present study has intended to extract nano calcium carbonate from the naturally available dolomite rock through the simple biomimetic synthesis. The basic characterization of the current sample has been reported [10]. The synthesized material was characterized through FTIR, XRD, FE-SEM, EDX-mapping and HR-TEM. The nanomaterial was also evaluated for the antibacterial and anticancer activities against *Staphylococcus aureus* and *Salmonella* sp. strains and MCF-7 cancer cell, respectively.

## EXPERIMENTAL

Natural carbonate source like dolomite rock ($CaMg(CO_3)_2$) (approximately 5 Kg) were collected from Arisipalayam village, Salem district, India. For synthesis, sucrose, anhydrous sodium carbonate and HCl were acquired from Sigma-Aldrich, USA. All the chemicals were of analytical grade with ≥ 99 % purity. The glasswares were washed thoroughly with nitric acid followed by deionized water. All dilution and sample preparation were carried out using ultrapure water.

**Preparation of nano $CaCO_3$:** The selection of samples, cleaning process of samples and synthesis procedure of nano $CaCO_3$ were done according to the reported method [10,11].

**Characterization:** The mineralogical and functional groups of the samples were analyzed through Fourier Transform Infrared (FT-IR) spectrometer (SHIMADZU-8400). The X-ray diffractometer (X'pertPRO) was utilized to analyze the purity and crystalline properties. The morphology and microstructure of the product were analyzed through Field Emission Scanning Electron Microscopy (CARL ZEISS-SIGMA-300) and High-Resolution Transmission Electron Microscopy (HR-TEM) [FEI, model: TECNAI G2-20TWIN] and X-ray photoelectron spectrometer (XPS) (Thermo Scientific K -Alpha; monochromatic Al*K*α radiation energy 1486.6 eV) was used to evaluate the chemical state.

**Antibacterial activity:** The inoculums was standardized at $1 \times 10^6$ CFU/mL and compared with turbidity standard (0.5 MacFarland tube). A source of cotton wool swabs was arranged on wooden applicator sticks. They were treated in culture tubes, tins, on paper in the autoclave. The agar disc diffusion method was followed for assessing antibacterial activity [12]. In present study, *Staphylococcus aureus* and *Salmonella* sp. bacterial strains were used. Muller-Hinton Agar (MHA) medium was dispensed in to the petriplate. Subsequently, the medium was hardened, the inoculums were spread on the MHA plates with sterile swab humidified with the bacterial holdup. Sterile samples (disc form) and 20 µL of standard antibiotic (ampicillin) disc were placed in MHA plates. The plates were incubated at 37 ºC for 24 h. The antibacterial activity was determined by measuring the diameter of zone of inhibition.

**Antiancer activity**

**Cell line and culture:** The MCF-7 cells were preserved in minimal essential medium accompanied with 10% FBS, penicillin (100 U/mL) and streptomycin (100 µg/mL) in a humidified atmosphere of 50 µg/mL $CO_2$ at 37 ºC. Minimum essential medium (MEM) was acquired from Hi Media Laboratories. Fetal bovine serum (FBS) was procured from Cistron Biological Laboratory, Coimbatore, India

The cells ($1 \times 10^5$/well) were plated in 24-well plates and incubated in 37 ºC with 5% $CO_2$ condition. The various concentrations of the sample, which were gradually diluted, were introduced and incubated for 24 h following the attainment of cell confluence. Then, the samples were detached from the well and washed with phosphate-buffered saline (pH 7.4) or MEM without serum. A 100 µL/well (5 mg/mL in PBS) of 0.5% MTT was added and incubated for 4 h followed by the addition of 1 mL of DMSO. The UV- spectrophotometer was utilized to record the absorbance at 570 nm by DMSO (blank) [13]. The measurements were executed and the concentration required for a 50% inhibition ($IC_{50}$) was evaluated. The following formula was used to calculate % cell viability:

$$\text{Cell viability (\%)} = \frac{\text{Treated cells}}{\text{Control cells}} \times 100$$

## RESULTS AND DISCUSSION

**FTIR:** The functional group analysis of nano $CaCO_3$ is shown in Fig. 1. The existences of the characteristic major and minor peaks at 710 ($\nu_4$), 875 ($\nu_2$), 1423 ($\nu_3$), 1796 ($\nu_1 + \nu_4$) and 2512 ($\nu_1 + \nu_3$) $cm^{-1}$ confirmed the presence of $CaCO_3$ [14]. The presences of well sharped and high intense peaks show that the synthesized sample composed of $CaCO_3$without any impurities [8]. The peak at 3420 $cm^{-1}$ is due to the OH stretching mode of hydroxyl group [15].

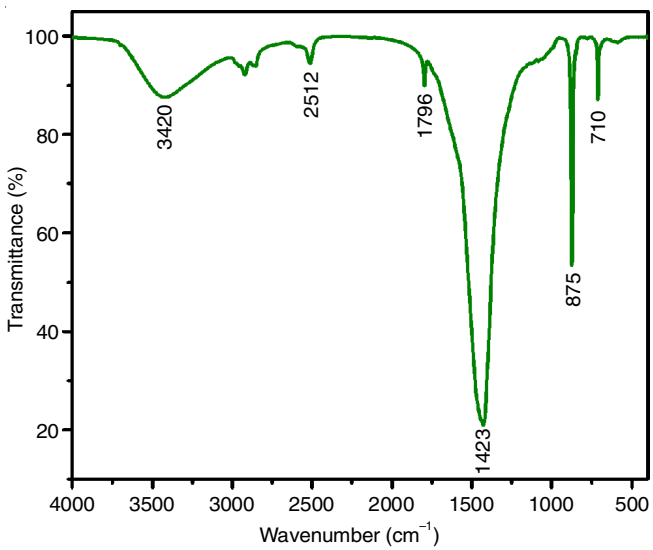


Fig. 1. FTIR spectrum of nano $CaCO_3$

**XRD:** The XRD patterns of nano $CaCO_3$ are shown in Fig. 2. The diffraction planes are observed at (0 1 2), (1 0 4), (0 0 6), (1 1 0), (1 1 3), (2 0 2), (0 1 8), (1 1 6), (1 1 2) and (1 1 9) with corresponding the 2θ values 22.97º, 29.34º, 31.35º, 35.89º, 39.33º, 43.07º, 47.49º, 48.44º, 57.30º and 60.65º. These planes are well coordinated with the rhombohedral calcite polymorphs ($CaCO_3$) (JCPDS No: 86-2343). It is observed that presence of planes are only belongs to calcite. From the observed 2θ values, the average crystallite size was calculated by Scherrer's formula [11] and the calculated size is found to be 25 nm.

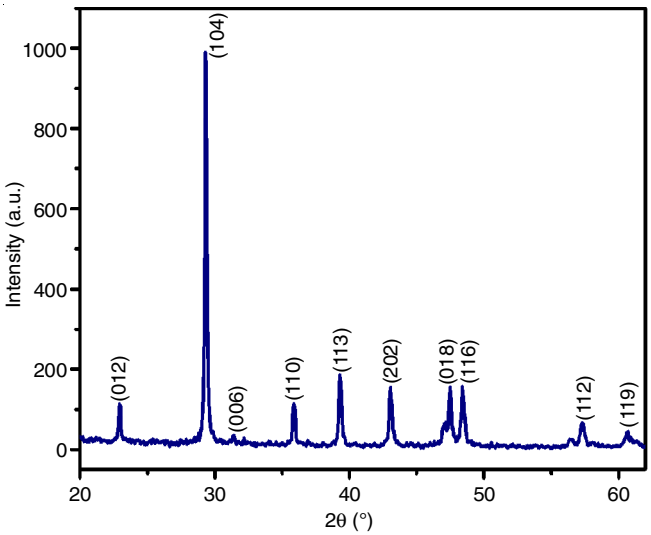


Fig. 2. XRD pattern of nano $CaCO_3$

**Morphological studies:** Fig. 3 shows the morphology of nano $CaCO_3$, where the rhombohedral crystal-like morphology was observed. The HR-TEM micrograph of nano $CaCO_3$ is shown in Fig. 4. From the result, all the particles are in spherical with few rhombohedral like nanoparticles. According to Sayed *et al.* [16], it is noteworthy to mention that there has been significant impact of metal oxide nanoparticle size and shape on their antibacterial properties. According to Cheon *et al.* [17] triangular plates exerted the lowest zone of bacterial growth inhibition, whereas spherical silver nanoparticles had the most powerful antibacterial action, followed by disc-shaped nanoparticles. Variations in the size and shape of the particles were identified as the cause of antibacterial activity. In spherical nanoparticles, greatest surface area and lowest size are observed, which support their increased antibacterial activities. Also, the spherical nanoparticles exhibit superior antibacterial activity at the lower minimal inhibitory doses [16].

**XPS:** Fig. 5a-d illustrates the XPS spectra of nano $CaCO_3$. The peaks Ca, C and O are observed in the spectrum of pure nano $CaCO_3$ (Fig. 5a) and demonstrated that they are all the constituents of the studied sample. Fig. 5b depicts the Ca 2p core spectrum with two strong peaks (350.88 and 347.32 eV) matching to $Ca^{2+}$ oxidation state ($2p_{1/2}$ and $2p_{3/2}$), respectively [18]. Five peaks are observed in the C 1s (Fig. 5c). Due to the atmospheric organic carbon (C–C/C–H bonding), a peak at 284.05 eV is presented. Other four peaks are observed at 285.32 (C–C), 286.55 (C–O–C/C–OH), 289.05 (C–O) and 290.08

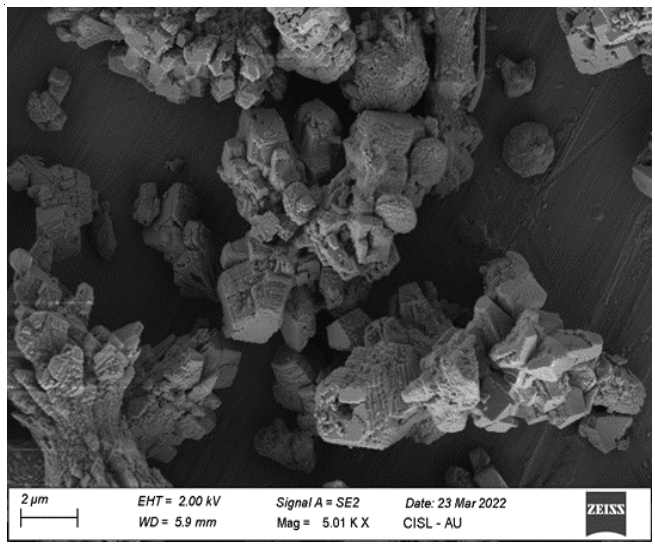


Fig. 3. FE-SEM images of nano $CaCO_3$

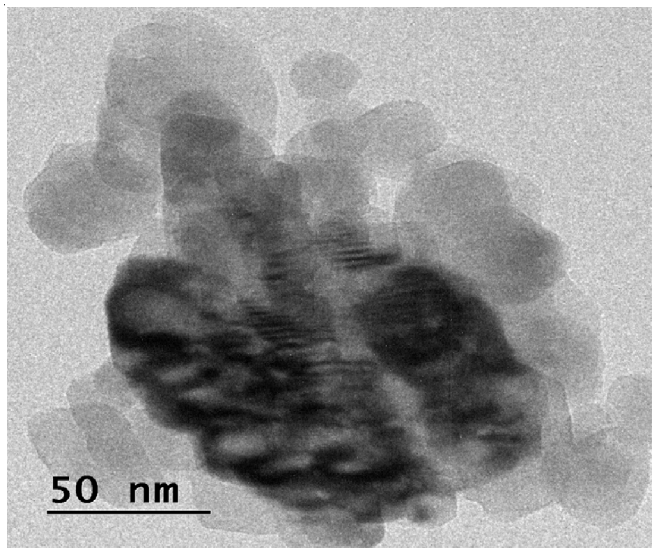


Fig. 4. HR-TEM images of nano $CaCO_3$

($CO_2$/C–C=O) eV [19,20]. Five deconvoluted peaks of O 1s such as 529.85, 531.85, 532.03, 533.42 and 534.35 eV are observed due to C=O, M-O, Ca-OH, O-H/C-O-C and $H_2O$/O-H bonding, respectively (Fig. 5d) [21]. From the above analysis, the presence of binding energy of Ca, C and O shows that the prepared product is in the pure form of $CaCO_3$.

**Antibacterial activity:** Antibacterial activity of $CaCO_3$ nanoparticles was assessed by calculating the inhibition zone against Gram-positive *Staphylococcus aureus* and Gram-negative *Salmonella* sp. bacteria strain. The $CaCO_3$ nanoparticles exhibit notable antibacterial activity against tested strains at 1000 µg/mL when compared with standard ampicillin (20 µL/mg) (Table-1). It showed the least activity 7 mm and 4 mm at 500 µg/mL. Among the studied strains, *Staphylococcus aureus* shows the highest sensitivity. Thus, it can be deduced that the disintegrate of the bacterial cell membrane and subsequent ejection of cytoplasmic material (bacteria death) may be the cause of suppression of bacterial growth by $CaCO_3$ nanoparticles [22]. When the nano $CaCO_3$ get into contact with bacterial cells,

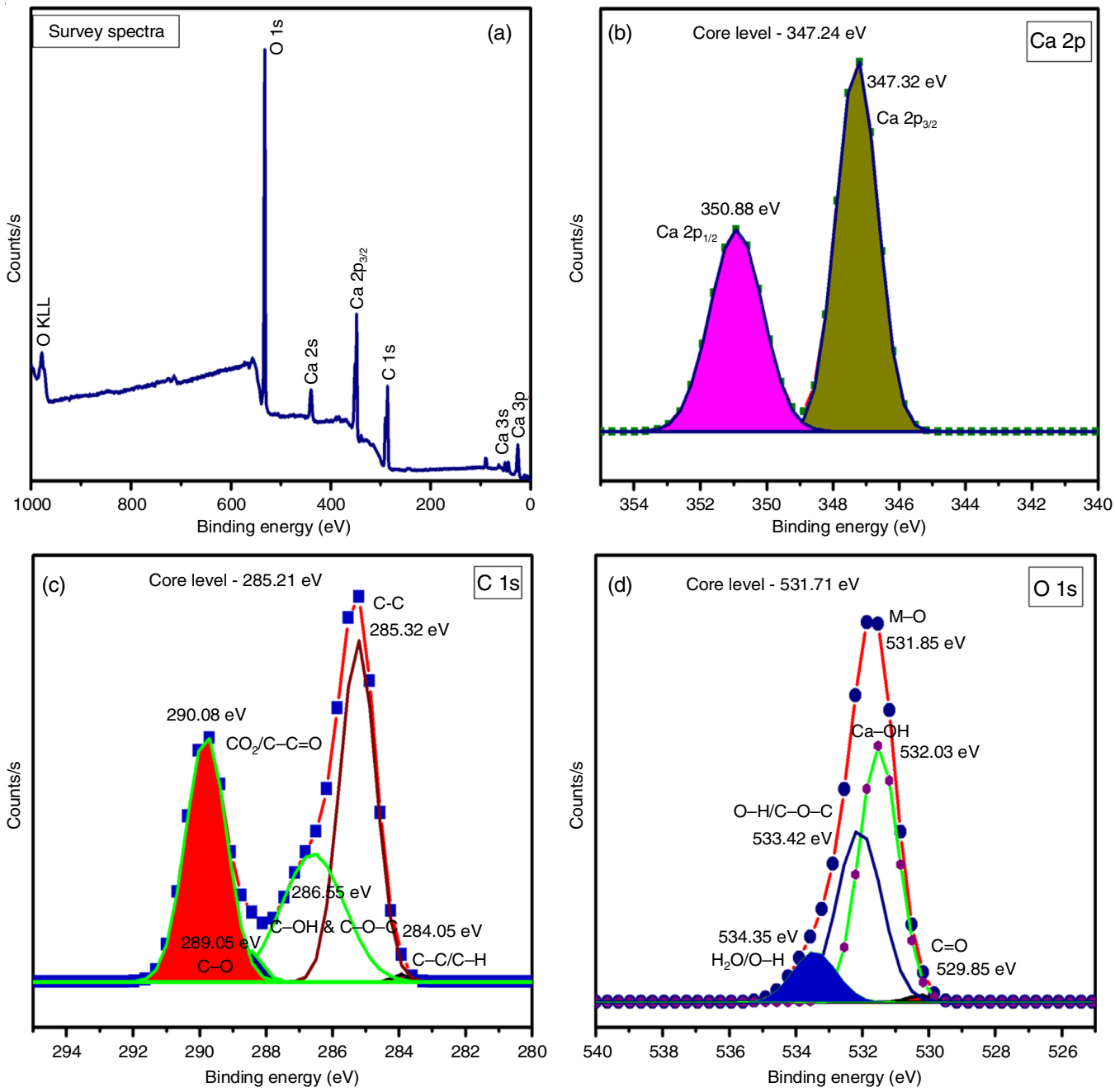


Fig. 5. X-ray photoelectron spectrum of nano $CaCO_3$ (a) survey spectrum, (b) Ca 2p region, (c) C 1s region and (d) O 1s region

TABLE-1
ANTIBACTERIAL ACTIVITY OF $CaCO_3$ NANOPARTICLES

| Bacterial strain | Zone of inhibition (mm) | | | |
|---|---|---|---|---|
| | 500 µg/mL | 750 µg/mL | 1000 µg/mL | Control |
| *S. aureus* | 07 | 08 | 09 | 11 |
| *Salmonella* sp. | 04 | 07 | 07 | 09 |

they mainly interact with the outer surface of plasma membranes. This action ultimately affects the plasma membranes penetrability by distrubing its stability. By penetrating the cytoplasmic interface, the disintegration of the membrane structure and the resulting development of $CaCO_3$ nanoparticles disrupt the fundamental process of cell development [23-25].

**Anticancer activity:** *In vitro* cytotoxic effect of $CaCO_3$ nanoparticles was evaluated against the chosen human cancer cell line MCF-7 (breast) using the MTT assay at various concentrations (7.8, 15.6, 31.2, 62.5, 125, 250, 500 and 1000 µg/mL) of the nanoparticles. The growth and proliferation of MCF-7 cell was found to be significantly inhibited by $CaCO_3$ nanoparticles. The cytotoxic effect of prepared $CaCO_3$ nanoparticles (7.8-1000 µg/mL) for 24 h is shown in Fig. 6a-e. It was found that the untreated control cells morphology was intact and normal, which clearly shows that $CaCO_3$ nanoparticles induce apoptosis in MCF-7 by reacting in a similar manner. Cell viability was influenced by $CaCO_3$ nanoparticles concentrations and decreased with increasing $CaCO_3$ nanoparticles (Table-2).

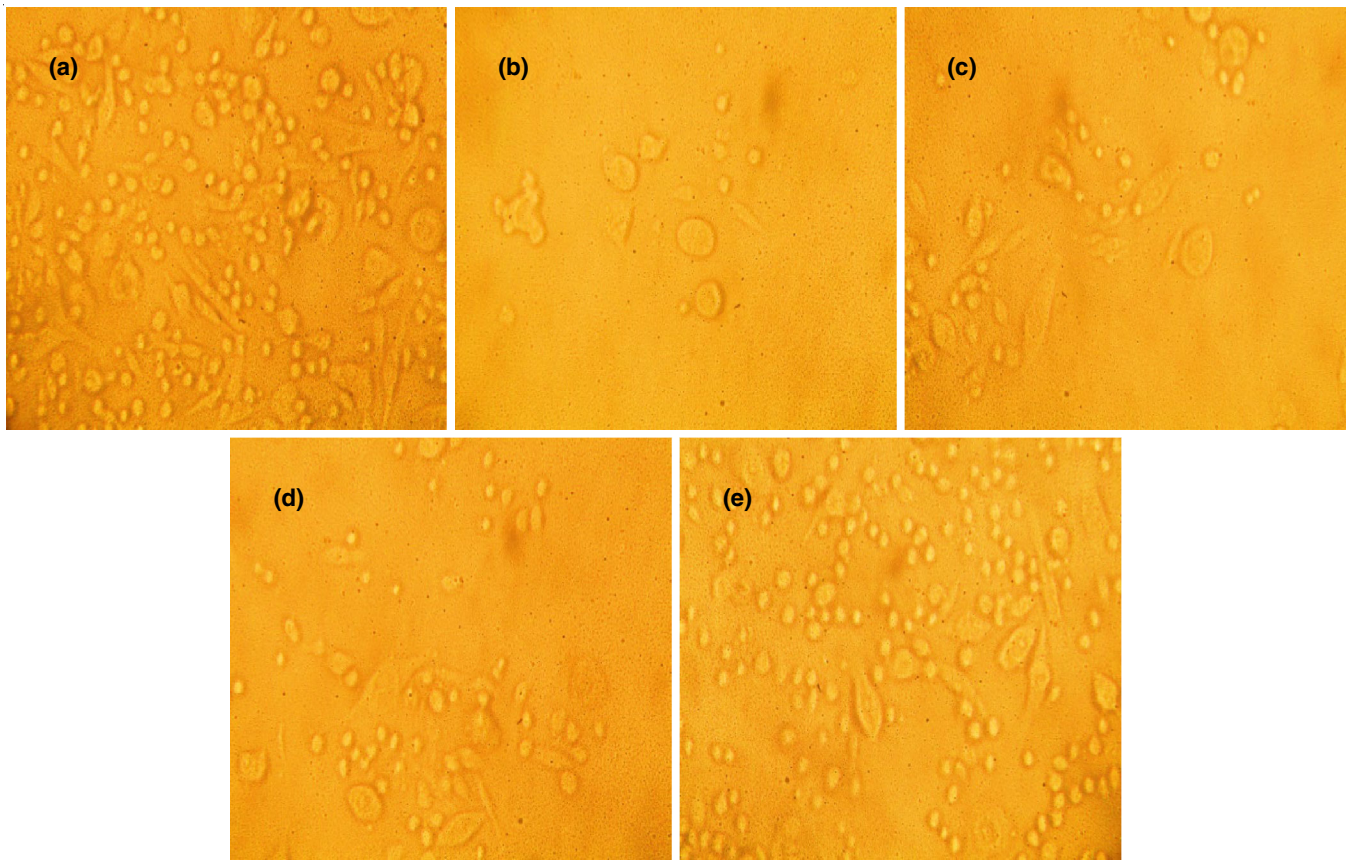


Fig. 6. Light microscope images of nano $CaCO_3$ against MCF-7 cell, (a) normal MCF-7 cell line, (b) toxicity at 1000 µg/mL, (c) toxicity at 250 µg/mL, (d) toxicity at 125 µg/mL and (e) toxicity at 62.5 µg/mL

TABLE-2
ANTICANCER EFFECT OF $CaCO_3$ NANOPARTICLES ON MCF-7 CELL LINE (24 h)

| Concentration (µg/mL) | Dilutions | Absorbance (O.D.) | Cell viability (%) |
|---|---|---|---|
| 1000 | Neat | 0.11 | 18.96 |
| 500 | 1.1 | 0.20 | 34.48 |
| 250 | 1.2 | 0.28 | 48.27 |
| 125 | 1.4 | 0.34 | 58.62 |
| 62.5 | 1.8 | 0.40 | 68.96 |
| 31.2 | 1.16 | 0.46 | 79.31 |
| 15.6 | 1.32 | 0.51 | 87.93 |
| 7.8 | 1.64 | 0.54 | 93.10 |
| Cell control | – | 0.58 | 100 |

The findings demonstrated that in comparison to the untreated control, cell viability decreased in a concentration dependent manner. The highest concentration was associated with distorted shape, shrinkage, detachment and disruption of membrane (Fig. 6b). At 1000 µg/mL, the number of viable cells was lowest level (18.96%) and at 7.8 µg/mL, it showed the highest level (93.10%). The synthesized product exhibits efficient against the MCF-7 cell but they were especially effective when the $CaCO_3$ nanoparticles was present.

The $IC_{50}$ value of $CaCO_3$ nanoparticles was determined and found to be 229.10 µg/mL (Fig. 7). Hammadi *et al.* [26], measured the cytotoxicity potential of $CaCO_3$ nanoparticles against MCF-7 cell after 72 h. It was found to be more than 86%. Also, they reported that the concentration of $CaCO_3$ nanoparticles increases with decreasing the cell viability of MCF-7 cell because the possible cellular uptake of the nanoparticles by the cell. Based on this result, the biomimetically prepared $CaCO_3$ nanoparticles exhibits good anticancer activity (81.04% at 24 h) against human breast cancer cell line (MCF-7 cell).

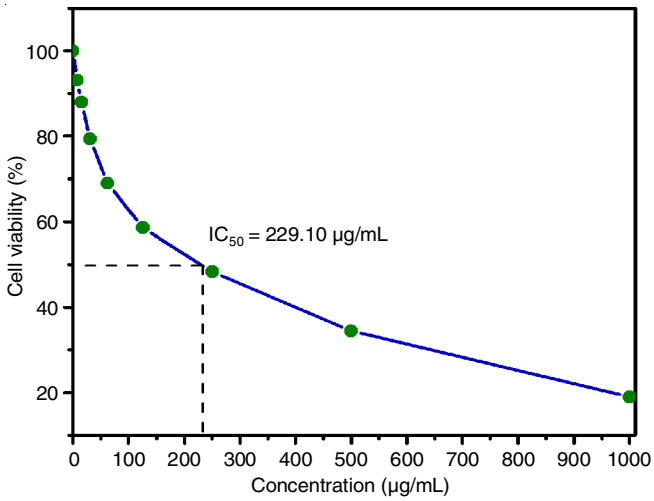


Fig. 7. $IC_{50}$ value of nano $CaCO_3$ against MCF-7 cell

## Conclusion

In summary, a facile, low-cost and eco-friendly biomimetic process has been developed to synthesize $CaCO_3$ nanoparticles from natural dolomite rock. $CaCO_3$ nanoparticles were charac-

terized for their functional group, structural, elemental and morphological analyses. The FTIR and XRD results suggested the crystalline in nature with rhombohedral calcite polymorphs with a crystallite size of 25 nm. Morphology studies showed that nanomaterials were in rhombohedral crystals like spherical nanoparticles. The XPS results of $CaCO_3$ nanoparticles showed that the obtained binding energies (Ca 2p, C 1s and O 1s) were in good agreement with $CaCO_3$. The nano $CaCO_3$ exhibited the good antimicrobial as well as anticancer agents for both Gram-positive (9 mm at 1000 µg/mL) and Gram-negative (7 mm at 1000 µg/mL) bacteria and human breast cancer cell line MCF-7. Therefore, the results concluded that the biomimetic synthesis of $CaCO_3$ nanoparticles can be used in biomedical applications.

## CONFLICT OF INTEREST

The authors declare that there is no conflict of interests regarding the publication of this article.

## REFERENCES


1. D. Render, T. Samuel, H. King, M. Vig, S. Jeelani, R.J. Babu and V. Rangari, *J. Nanomater.*, **2016**, 3170248 (2016); https://doi.org/10.1155/2016/3170248
2. C. Tan, C. Dima, M. Huang, E. Assadpour, J. Wang, M.S. Kharazmi, B. Sun, and S.M. Jafari, *Adv. Colloid Interface Sci.*, **309**, 102791 (2022); https://doi.org/10.1016/j.cis.2022.102791
3. Y.-Q. Niu, J.-H. Liu, C. Aymonier, S. Fermani, D. Kralj, G. Falini and C.-H. Zhou, *Chem. Soc. Rev*., **51**, 7883 (2022); https://doi.org/10.1039/D1CS00519G
4. M.H. Azarian and W. Sutapun, *Front. Mater.*, **9**, 1024977 (2022); https://doi.org/10.3389/fmats.2022.1024977
5. P. Zhao, Y. Tian, J. You, X. Hu and Y. Liu, *Bioengineering*, **9**, 691 (2022); https://doi.org/10.3390/bioengineering9110691
6. X. Yang, Y. Sun, H. Zhang, F. Liu, Q. Chen, Q. Shen, Z. Kong, Q. Wei, J.-W. Shen and Y. Guo, *Nanoscale*, **16**, 6876 (2024); https://doi.org/10.1039/D3NR05986C
7. N.S. Alduraihem, R.S. Bhat, S.A. Al-Zahrani, D.M. Elnagar, H.M. Alobaid and M.H. Daghestani, *Processes*, **11**, 301 (2023); https://doi.org/10.3390/pr11020301
8. V. Ramasamy, P. Anand and G. Suresh, *Adv. Powder Technol.*, **29**, 818 (2018); https://doi.org/10.1016/j.apt.2017.12.023
9. S.F.A. Abdullah, S.S.M. Saleh, N.F. Mohammad, M.S. Idris and H.R. Saliu, *J. Phys.: Conf. Ser.*, **2080**, 012009 (2021); https://doi.org/10.1088/1742-6596/2080/1/012009
10. R. Venkidasamy, T. Elumalai, S. Govindhasamy, S. Tharmalingam and J.J.S. Emmanuel Rajan, *Chem. Eng. Commun.*, **211**, 229 (2024); https://doi.org/10.1080/00986445.2023.2233002
11. V. Ramasamy, E. Thenpandiyan, G. Suresh, T. Sathishpriya and S. Sagadevan, *Opt. Mater.*, **142**, 114130 (2023); https://doi.org/10.1016/j.optmat.2023.114130
12. A. Roy, S.S. Gauri, M. Bhattacharya and J. Bhattacharya, *J. Biomed. Nanotechnol.*, **9**, 1 (2013); https://doi.org/10.1166/jbn.2013.1681
13. V. Popova, Y. Poletaeva, A. Chubarov and E. Dmitrienko, *Pharmaceutics*, **15**, 771 (2023); https://doi.org/10.3390/pharmaceutics15030771
14. V. Ramasamy, T. Sathishpriya, E. Thenpandiyan, G. Suresh and S. Sagadevan, *Inorg. Chem. Commun.*, **155**, 111062 (2023); https://doi.org/10.1016/j.inoche.2023.111062
15. H.H. Adler and P.F. Kerr, *Am. Mineral.*, **48**, 839 (1963).
16. F.A.Z. Sayed, N.G. Eissa, Y. Shen, D.A. Hunstad, K.L. Wooley and M. Elsabahy, *J. Nanobiotechnology*, **20**, 536 (2022); https://doi.org/10.1186/s12951-022-01733-x
17. J.Y. Cheon, S.J. Kim, Y.H. Rhee, O.H. Kwon and W.H. Park, *Int. J. Nanomedicine*, **14**, 2773 (2019); https://doi.org/10.2147/IJN.S196472
18. T. Roychowdhury, S. Bahr, P. Dietrich, M. Meyer, A. Thißen and M.R. Linford, *Surf. Sci. Spectra*, **26**, 014025 (2019); https://doi.org/10.1116/1.5109266
19. Q. Wang, Y. Wang, J. Tang, Z. Yang, L. Zhang and X. Huang, *Chemosphere*, **303**, 135048 (2022); https://doi.org/10.1016/j.chemosphere.2022.135048
20. S. Thakur, J. Chaudhary, A. Thakur, O. Gunduz, W.F. Alsanie, C. Makatsoris and V.K. Thakur, *Chemosphere*, **303**, 134917 (2022); https://doi.org/10.1016/j.chemosphere.2022.134917
21. L. Wang, J. Wang, Z. Wang, C. He, W. Lyu, W. Yan and L. Yang, *Chem. Eng. J.*, **354**, 623 (2018); https://doi.org/10.1016/j.cej.2018.08.074
22. R. Dobrucka and J. Dlugaszewska, *Saudi J. Biol. Sci.*, **23**, 517 (2016); https://doi.org/10.1016/j.sjbs.2015.05.016
23. R. Sinha, R. Karan, A. Sinha and S.K. Khare, *Bioresour. Technol.*, **102**, 1516 (2011); https://doi.org/10.1016/j.biortech.2010.07.117
24. P.K. Stoimenov, R.L. Klinger, G.L. Marchin and K.J. Klabunde, *Langmuir*, **18**, 6679 (2002); https://doi.org/10.1021/la0202374
25. L. Zhang, Y. Jiang, Y. Ding, M. Povey and D. York, *J. Nanopart. Res.*, **9**, 479 (2007); https://doi.org/10.1007/s11051-006-9150-1
26. N.I. Hammadi, Y. Abba, M.N.M. Hezmee, I.S.A. Razak, A.Z. Jaji, T. Isa, S.K. Mahmood and M.Z.A.B. Zakaria, *Pharm. Res.*, **34**, 1193 (2017); https://doi.org/10.1007/s11095-017-2135-1